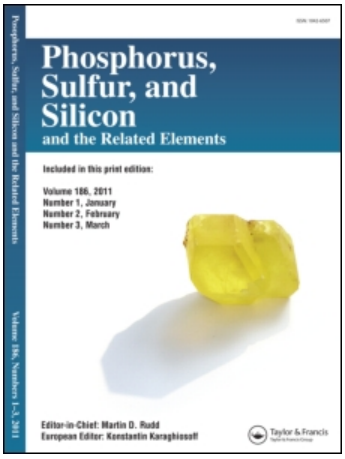

Phosphorus, Sulfur, and Silicon and the Related Elements
Publication details, including instructions for authors and subscription information:
http://www.informaworld.com/smpp/title~content=t713618290

P(O, S, Se, and Te)-π(Ar) Conjugations as Factors to Control Fine Structures of 1-(Chalcogena)naphthalenes

Takahito Nakai[a]; Satoko Hayashi[a]; Waro Nakanishi[a]
[a] Department of Material Science and Chemistry, Faculty of Systems Engineering, Wakayama University, Wakayama, Japan

Online publication date: 27 May 2010

To cite this Article Nakai, Takahito , Hayashi, Satoko and Nakanishi, Waro(2010) 'P(O, S, Se, and Te)-π(Ar) Conjugations as Factors to Control Fine Structures of 1-(Chalcogena)naphthalenes', Phosphorus, Sulfur, and Silicon and the Related Elements, 185: 5, 1031 — 1045
To link to this Article: DOI: 10.1080/10426501003772235
URL: http://dx.doi.org/10.1080/10426501003772235

Phosphorus, Sulfur, and Silicon, 185:1031–1045, 2010

ISSN: 1042-6507 print / 1563-5325 online
DOI: 10.1080/10426501003772235

Taylor & Francis
Taylor & Francis Group

P(O, S, Se, AND Te)–π(Ar) CONJUGATIONS AS FACTORS TO CONTROL FINE STRUCTURES OF 1-(CHALCOGENA)NAPHTHALENES

Takahito Nakai, Satoko Hayashi, and Waro Nakanishi
Department of Material Science and Chemistry, Faculty of Systems Engineering, Wakayama University, Wakayama, Japan

The p(Z)–π(Ar) conjugation as the factors to control the fine structures of organic chalcogen compounds are investigated. The structures of 1-(arylchalcogena)naphthalenes [1-(p-$YC_6H_4Z)C_{10}H_7$, 1-ArZNap; 1 (Z = O) and 2 (Z = S)] are determined by the X-ray crystallographic analysis. The structures of 1, 2, and 1-ArTeNap (4) are also determined in solutions, together with 1-ArSeNap (3), employing the NMR data of 9-(arylselanyl)anthracenes (5) and 1-(arylselanyl)anthraquinones (6). NMR data of 5 and 6 can be used as the standard of the A and B structures, respectively, for all Y examined in solutions: The Se–C_{Ar} bond in 5 (A) is placed almost perpendicular to the anthryl plane in A, and the bond is located on the plane in 6 (B). Structures of 1–4 are A if Y are electronically accepting groups such as Y = Cl, but they are B with Y of donating groups such as Y = OMe both in crystals and solutions. It is interesting that δ(C_i: 1–4) are hardly affected from the conformation around the Z–C_{Ar} bonds, whereas δ(H: 1–4) and δ(Se: 3) change depending on the conformation, which enables us to determine the conformations.

Keywords 1-(Arylchalcogena)naphthalenes; lone pairs; structure; substituent dependence; through-bond interactions

INTRODUCTION

Factors to control the fine structures of organic chalcogen compounds are of current interest in relation to the p–π conjugation of the p(Z)–π(Ar) type[1] such as in 1-(arylchalcogena)naphthalenes [1-(*p*-$YC_6H_4Z)C_{10}H_7$, 1-ArZNap; **1** (Z = O), **2** (Z = S), **3** (Z = Se),[2–5] and **4** (Z = Te)] (Chart 1). Do the p(Z)–π(Ar) conjugations really control the fine structures of **1**–**4**, while the conjugation is believed to decrease swiftly as Z becomes heavier? The role of the p(Z)–π(Ar) conjugation is to clarified as the factor to control the fine structures of **1**–**4**.

Received 29 November 2008; accepted 28 December 2008.
Dedicated to Professor Naomichi Furukawa on the occasion of his 70th birthday.
We thank K. Takada for technical assistance in the preparations. This work was partially supported by a Grant-in-Aid for Scientific Research (Nos. 16550038, 19550041, and 20550042) from the Ministry of Education, Culture, Sports, Science and Technology, Japan.
Address correspondence to Waro Nakanishi, Department of Material Science and Chemistry, Faculty of Systems Engineering, Wakayama University, 930, Sakaedani, Wakayama 640–8510, Japan. E-mail: nakanisi@sys.wakayama-u.ac.jp

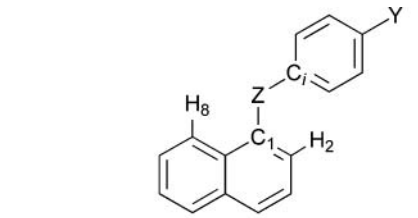

	1	2	3	4
Z =	O	S	Se	Te

	a	b	c	d	e	f	g	h	i	j
Y =	H	NMe_2	OMe	Me	F	Cl	Br	COOEt	CN	NO_2

Chart 1

The type **A** (**A**), **B**, and **C** notation[2,6,7] is proposed for the naphthyl group of **3** to specify the fine structure, together with the planar (**pl**), perpendicular (**pd**), and the nonplanar and nonperpendicular (**np**) notation for the aryl group.[8,9] The Se–C_{Ar} bond in **3** is placed almost perpendicular to the naphthyl plane in **A**, the bond is located on the plane in **B**, and **C** is the intermediate between **A** and **B**. The Se–C_{Nap} bond in **3** is placed almost perpendicular to the naphthyl plane in **pd**, the bond is located on the plane in **pl**, and **np** is the intermediate between **pd** and **pl**. Scheme 1 shows the **A**, **B**, and **C** notation exemplified by 8-G-1-$XZC_{10}H_6$ and the **pl**, **pd**, and **np** conformers in C_6H_5ZX. The combined notation will be used for the structures of **1**–**4**: It is called (**A**, **pl**) if the Z–C_{Ar} bond is almost perpendicular to the naphthyl plane (**A**) and the Z–C_{Nap} bond is located on the aryl plane (**pl**), for example.

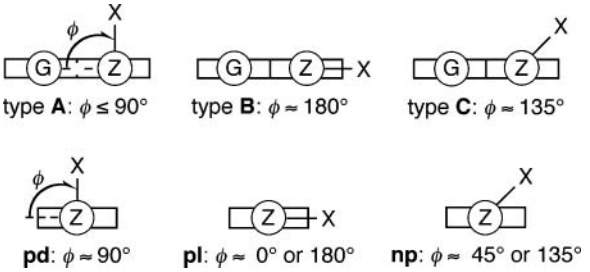

Scheme 1 Types A–C notation in naphthalene system and pd, pl, and np in benzene system.

Structures of **3** in crystals and/or solutions are reported for Y = H (**a**), NMe_2 (**b**), OMe (**c**), Me (**d**), F (**e**), Cl (**f**), Br (**g**), COOEt (**h**), CN (**i**), and NO_2 (**j**).[2–4] Those of **3c** and **3g** are displayed in Figure 1.[2] The structures are apparently (**B**, **pd**) for **3c** and (**A**, **pl**) for **3g** in crystals. The structures of **3** are demonstrated to change dramatically depending on Y in crystals. Structures of **3** in solutions are determined employing ^{77}Se NMR chemical shifts (δ(Se)) of 9-(arylselanyl)anthracenes (**5**: *p*-YC_6H_4SeAtc) and 1-(arylselanyl)anthraquinones (**6**: 1-(*p*-YC_6H_4Se)Atq) (Chart 2).[3] Structures of **5** and **6** are demonstrated to be (**A**, **pl**) and (**B**, **pd**), respectively, for all Y examined in solutions where

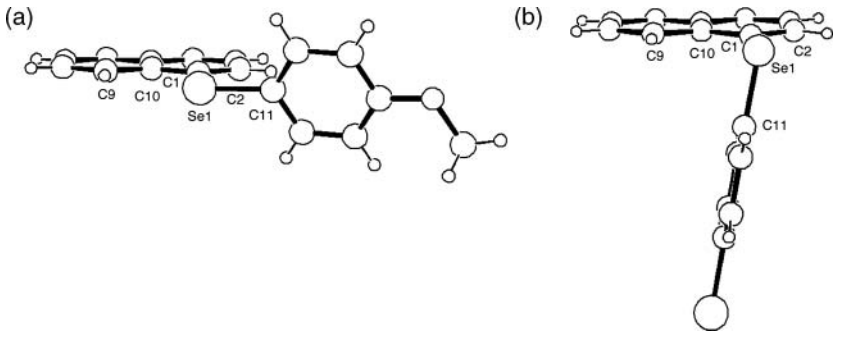

Figure 1 Structures of **3c** (a) and **3g** (b) with atomic numbering scheme for selected atoms.

a–**j**.[3,10] NMR data of **5** (**A**, **pl**) and **6**(**B**, **pd**) will be employed to determine the structures of **1**–**4** in solutions.

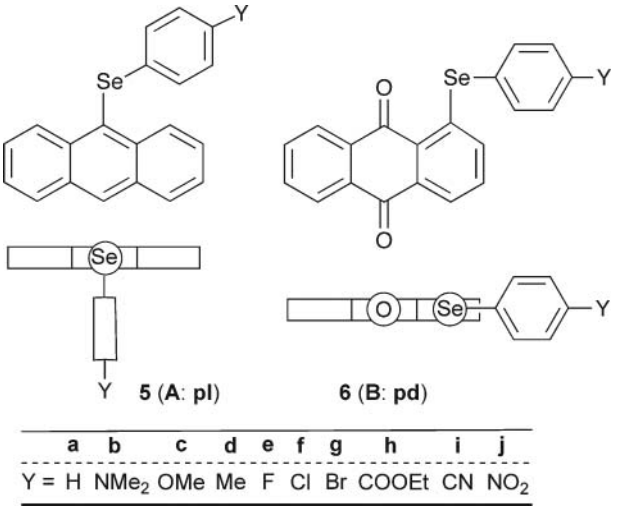

Chart 2

Chalcogenides **1**,[11] **2**, and **4** are prepared for **a**, **c, d**, **f**–**h**, and **j**. The structures in crystals are determined for some of **1** and **2** by the X-ray crystallographic analysis. The structures in solutions are also investigated employing the NMR data of **1**, **2**, and **4**, together with **5** and **6**. The results are analyzed, together with those of **3**, to clarify the role of the p(Z)–π(C_6H_4)–p(Y) conjugation as the factor to control the fine structures.

RESULTS AND DISCUSSION

Structure of 1-ArZNap (Z = O, S, and Se) in Crystals

Single crystals of **1** and **2** were obtained via slow evaporation of hexane solutions, and one of the suitable crystals was subjected to X-ray crystallographic analysis for each compound.[12] Only one type of structure corresponds to each of them in the crystal. Figure 2

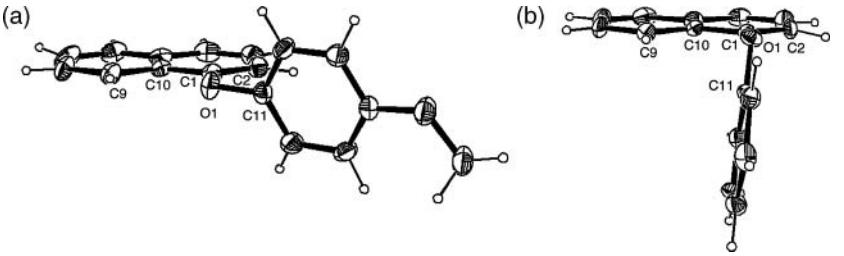

Figure 2 Structures of **1c** (a) and **1a** (b) with atomic numbering scheme for selected atoms (thermal ellipsoids are shown at the 40% probability level).

shows the structures of **1a** and **1c**, and Figure 3 shows those of **2c** and **2g**. The structures of **3c** and **3g** are determined by the X-ray crystallographic analysis are displayed in Figure 1.[2] The structures of **1c** and **2c** are essentially the same as that of **3c**, and the structures of **1a** and **2g** are very close to that of **3g**.

As shown in Figures 2 and 3, the planarity of the naphthyl, phenyl, *p*-anisyl, and *p*-bromophenyl planes in **1a**, **1c**, **2c**, and **2g** are very good. The *p*-anisyl plane in **1c** and **2c** were perpendicular to the naphthyl plane, the Se–C_{An} bonds are placed on the naphthyl plane, and the Se–C_{Nap} bonds are perpendicular to the *p*-anisyl plane: For **1c** and **2c**, the torsional angles of C2C1Z1C11 are –0.5° and 2.1°, respectively; those of C10C1Z1C11 are 179.2° and –179.1°, respectively; those of C1Z1C11C12 are 103.2° and 109.0°, respectively; and those of C1Z1C11C16 are –79.9° and –77.3°, respectively. The $C_{Nap}ZC_{An}$ angles (∠C1Z1C11) in **1c** and **2c** are 118.0° and 104.6°, respectively. Structures of **1c** and **2c** belong to (**B**, **pd**). On the other hand, the phenyl plane in **1a** and the *p*-bromophenyl plane in **2g** were perpendicular to the naphthyl plane, the Se–C_{Ar} bonds are perpendicular to the naphthyl plane, and the Se–C_{Nap} bonds are placed on the aryl plane: For **1a** and **2g**, the torsional angles of C2C1Z1C11 are –99.5° and 101.4°, respectively; those of C10C1Z1C11 are 84.4° and –79.3°, respectively; those of C1Z1C11C12 are –179.2° and 175.7°, respectively; and those of C1Z1C11C16 are 1.6° and –6.3°, respectively. The $C_{Nap}ZC_{Ar}$ angles (∠C1Z1C11) in **1a** and **2g** are 116.6° and 102.2°, respectively. Structures of **1a** and **2g** belong to (**A**, **pl**).

The results show that the structures of **1** and **2**, as well as those of **3**, are controlled by Y of the phenyl *para*-substituents. It shows that the structures of **1**–**3** will be (**B**, **pd**)

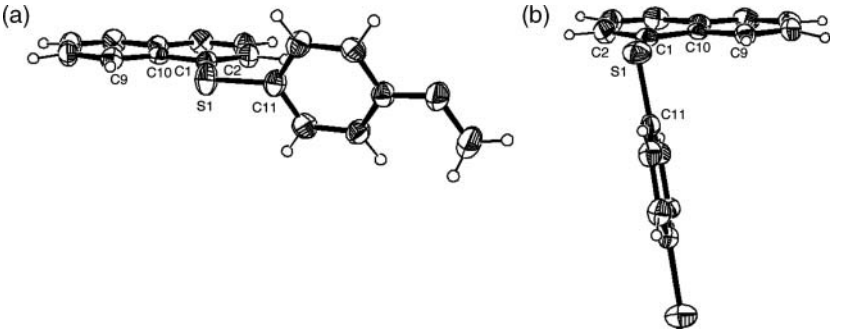

Figure 3 Structures of **2c** (a) and **2g** (b) with atomic numbering scheme for selected atoms (thermal ellipsoids are shown at the 40% probability level).

in crystals if Y is an electron-donating group, but they will be (**A**, **pl**) for Y of electron-accepting property. The driving force must be the energy stabilizing effect of the electrons in the p-type lone pair orbital of Z (p(Z)). The structure should be **A** if electrons in p(Z) are stabilized more effectively by the $\pi(C_6H_4Y)$ orbital with the electron accepting Y than by the π(Nap) orbital through the p(Z)–$\pi(C_6H_4Y/Nap)$ conjugation. It should be **B** when electrons in p(Z) are destabilized by the $\pi(C_6H_4Y)$ orbital with the electron donating Y, relative to the case with the π(Nap) orbital through the p(Z)–$\pi(C_6H_4Y/Nap)$ conjugation.

What factor controls the stability of (**A**, **pl**) and (**B**, **pd**)? Electron affinity of the components is proposed to determine the fine structures: The components are benzene, substituted benzenes, and naphthalene for **1**–**4**. The idea is proposed to evaluate the stability of **3**.[2] The structure should be **A** if the electrons in p(Z) are stabilized more effectively by the $\pi(C_6H_4)$–p(Y) orbital than by the π(Nap) orbital if the electron affinity of Y is substantially large, and vice versa. Scheme 2 illustrates the orbital interactions in **1**–**4**, where Y of accepting groups stabilize **A**, and Y of donating groups stabilize **B**. The idea would be applied to the factor to control the fine structures of **1** and **2**, as well as **3**.

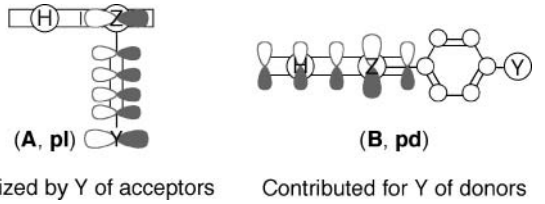

Scheme 2 The p(Z)–$\pi(C_6H_4)$–p(Y) conjugation to control the A and B conformers.

Indeed, the structures of **4** are not determined by the X-ray crystallographic analysis, but they could be determined in solutions by employing the NMR data of **5** and **6**: The structures of **5** and **6** are firmly demonstrated to be (**A**, **pl**) and (**B**, **pd**), respectively, for all Y examined in solutions.[3] The structures of **1**, **2**, and **4** are determined in solutions, and the factors to control the fine structures of **1**, **2**, and **4** are considered, together with those of **3**, next.

Structures of 1-ArZNap (1–4) in Solutions

Table I shows selected substituent-induced $\delta(H)_{SCS}$, $\delta(C)_{SCS}$, and/or $\delta(Se)_{SCS}$ values for **1**–**4**, together with those for **5** and **6**, measured in chloroform-*d* (0.050 mol/L) at 24°C. The $\delta(H_2)$, $\delta(H_8)$, $\delta(C_i)$, and/or δ(Se) values are also given for the parent compounds with Y = H (**1a**–**6a**) in parenthesis.

The rules of thumb, which are useful to discuss the structures of ArSeR in solutions based on δ(Se: **5**)$_{SCS}$ and δ(Se: **6**)$_{SCS}$ as the standards are summarized as follows: In the case of **5** (**A**, **pl**), large upfield and downfield shifts are observed for [**5c** (Y = OMe) and **5d** (Y = Me)] and [**5h** (Y = COOEt) and **5j** (Y = NO_2)], respectively. δ(Se: **5f** (Y = Cl)) and δ(Se: **5g** (Y = Br)) are very close to δ(Se: **5a** (Y = H)). For **6** (**B**, **pd**), only large upfield shifts are observed for **6c** (Y = OMe) and **6d** (Y = Me). δ(Se: **6h** (Y = COOEt)) is very similar to δ(Se: **6a** (Y = H)). δ(Se: **6i**: Y = CN) is more downfield of δ(Se: **6j**: Y = NO_2).

Following conclusions are obtained for **3**, by plotting δ(Se: **3**)$_{SCS}$ versus δ(Se: **5**)$_{SCS}$ and δ(Se: **6**)$_{SCS}$[13]: The structure of **3** should be exclusively (**A**, **pl**) for Y = NO_2 (**j**); however, the equilibrium between (**A**, **pl**) and (**B**, **pd**) contributes gradually in solutions as

Table I Substituent-induced chemical shifts (δ_{SCS}) of ^{1}H, ^{13}C, and/or ^{77}Se nuclei of **1–6**

	NMe_2 (**b**)	OMe (**c**)	Me (**d**)	H (**a**)	F (**e**)	Cl (**f**)	Br (**g**)	COOEt (**h**)	CN (**i**)	NO_2 (**j**)
1 (Z = O)										
$\delta(H_2)_{SCS}$		−0.063	−0.025	0.000 (7.602)[a]		0.003	0.011	0.118		0.182
$\delta(H_8)_{SCS}$		0.091	0.035	0.000 (8.201)[a]		0.021	0.000	−0.174		−0.272
$\delta(C_i)_{SCS}$		−7.2	−3.5	0.0 (157.9)[a]		−1.2	−0.6	4.5		6.1
2 (Z = S)										
$\delta(H_2)_{SCS}$		−0.288	−0.105	0.000 (7.652)[a]		0.024	0.040	0.200		0.286
$\delta(H_8)_{SCS}$		−0.001	0.000	0.000 (8.348)[a]		−0.053	−0.057	−0.074		−0.126
$\delta(C_i)_{SCS}$		−11.7	−4.4	0.0 (136.9)[a]		−1.2	−0.3	7.8		11.6
3 (Z = Se)										
$\delta(H_2)_{SCS}$	−0.467	−0.277	−0.108	0.000 (7.776)[a]	−0.101	0.003	0.021	0.096	0.113	0.125
$\delta(H_8)_{SCS}$	−0.088	−0.068	−0.021	0.000 (8.348)[a]	−0.053	−0.062	−0.059	−0.068	−0.101	−0.109
$\delta(C_i)_{SCS}$	−18.15	−11.48	−4.37	0.00 (131.66)[a]	−5.98	−1.55	−0.64	8.17	9.45	12.36
$\delta(Se)_{SCS}$	−17.2	−6.8	−4.8	0.0 (361.0)[a]	−5.0	−1.6	−1.7	7.0	13.8	18.6
4 (Z = Te)										
$\delta(H_2)_{SCS}$		−0.231	−0.092	0.000 (7.972)[a]		0.022	0.048	0.198		0.260
$\delta(H_8)_{SCS}$		−0.072	−0.053	0.000 (8.135)[a]		0.000	−0.005	0.065		0.142
$\delta(C_i)_{SCS}$		−11.8	−4.5	0.0 (114.7)[a]		−2.2	−1.0	8.1		12.0
5										
$\delta(H_1)_{SCS}$	0.127	0.045	0.005	0.000 (8.884)[a]	−0.028	−0.075	−0.084	−0.166	−0.186	−0.218
$\delta(H_{10})_{SCS}$	−0.077	−0.045	−0.019	0.000 (8.567)[a]	−0.008	0.008	0.010	0.071	0.060	0.103
$\delta(H_o)_{SCS}$	0.084	0.044	−0.068	0.000 (7.057)[a]	0.005	−0.073	−0.157	−0.017	−0.028	−0.007
$\delta(C_i)_{SCS}$	−8.13	−3.11	−1.13	0.00 (126.57)[a]	1.24	2.83	3.94	13.23	14.89	17.73
$\delta(Se)_{SCS}$	−21.0	−12.2	−6.6	0.0 (249.0)[a]	−3.6	1.5	1.6	16.2	26.2	30.3
6										
$\delta(H_2)_{SCS}$	0.102	0.023	0.024	0.000 (7.237)[a]	−0.038	−0.017	−0.012	−0.052	−0.056	−0.052
$\delta(H_8)_{SCS}$	0.024	0.022	0.013	0.000 (8.352)[a]	0.005	0.011	0.010	0.016	0.011	0.018
$\delta(H_o)_{SCS}$	−0.196	−0.102	−0.128	0.000 (7.724)[a]	−0.032	−0.071	−0.144	0.046	−0.009	0.196
$\delta(C_i)_{SCS}$	−13.87	−8.05	−2.06	0.00 (127.44)[a]	−3.45	2.21	2.21	5.26	5.27	5.66
$\delta(Se)_{SCS}$	−19.5	−15.0	−8.9	0.0 (512.3)[a]	−10.1	−7.0	−6.4	0.0	8.2	2.5

[a] $\delta(H)_{SCS}$, $\delta(C)_{SCS}$, and/or $\delta(Se)_{SCS}$ are given for **1–6**, together with $\delta(H)$, $\delta(C)$, and $\delta(Se)$ for **1a–6a** in parenthesis, measured in chloroform-*d* (0.050 mol/L) at 24°C.

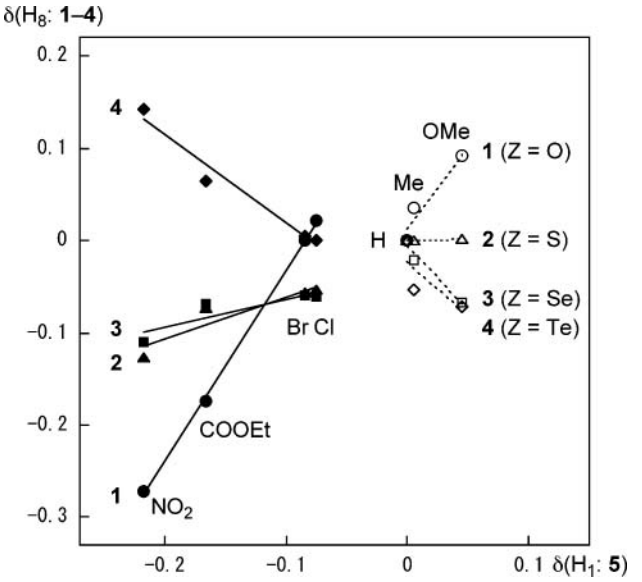

Figure 4 Plots of $\delta(H_8$: **1–4**) versus $\delta(H_1$: **5**).

the acceptor ability of Y becomes weaker, although the plot gives an excellent correlation for Y = NO_2 (**j**), CN (**i**), COOEt (**h**), Br (**g**), Cl (**f**), and F (**e**). (**B**, **pd**) would be predominant for Y = NMe_2 (**b**) (and Y = OMe (**c**)) in solutions. The equilibrium would substantially contribute to the structures of **3** with Y = H (**a**), Me (**c**), and halogens (**e–g**). Similar conclusions are obtained for the structures of **3** by employing ^{1}H and ^{13}C NMR chemical shifts.

The structures of **1**, **2**, and **4**, together with **3**, are investigated in solutions to determine the fine structures in solutions and consider the factors to control the fine structures. If a good correlation is obtained for some Y in the plot versus δ(H: **5**), the structure is expected to be (**A**, **pl**) in solutions for Y. The H_1 atom in **5** corresponds to H_8 in **1–4** and both H_1 in **5**, and H_2 in **1–4** are placed adjacent to Z. Therefore, $\delta(H_8)$ and $\delta(H_2)$ of **1–4** are plotted versus $\delta(H_1$: **5**). Figure 4 shows the plots of $\delta(H_8$: **1–4**) versus $\delta(H_1$: **5**). The plots are analyzed as two correlations for each: Y = OMe (**c**), Me (**d**), and H(**a**) make one group, and (G(**m**)) and Y = Cl (**f**), Br (**g**), COOEt (**h**), and NO_2 (**j**) belong to another group (G(**n**)). Table II shows the correlations separately by two groups [entries 1–4 for G(**m**) and entries 5–8 for G(**n**)]. Figure 5 shows the plots of $\delta(H_2$: **1–4**) versus $\delta(H_1$: **5**), which are analyzed by G(**m**) and G(**n**) for each, again. Table II shows the correlations separately by two groups [entries 9–12 for G(**m**) and entries 13–16 for G(**n**)].

Plots of $\delta(H_8$: **3**) versus $\delta(H_1$: **5**) in Figure 4 are discussed first, since Z for both **3** and **5** is Se. The correlation constant (*a*) is a positive value of 0.30 for G(**n**) (entry 7 in Table II), which is in accordance with **3** (**A**, **pl**) for G(**n**), although some equilibrium cannot be neglected for Y of halogens. The *a* values for G(**n**) in the plots of $\delta(H_8$: **1–4**) versus $\delta(H_1$: **5**) become smaller monotonically as Z goes from O (**1**), S (**2**), to Se (**3**), then to Te (**4**) (entries 5–8 in Table II). The trend is also in accordance with the (**A**, **pl**) structure for G(**n**) in **1–4**. The observed (**A**, **pl**) structures for **1a**, **2g**, and **3g** in crystals support the conclusion. On the other hand, the plots for G(**m**) gave another correlation for each (entries 1–4 in Table II): A negative value of $a = -1.38$ is predicted for G(**m**) of **3**, which must be the reflection of **3**

Table II Correlations in the plots of $\delta(H_2)$ and $\delta(H_8)$ for **1–4** versus those of **5**, analyzed separately by two groups for most cases[a]

Entries	Correlation	*a*	*b*	*r*	*n*(Y)	Group[b]
1	$\delta(H_8$: **1**$)_{SCS}$ *vs.* $\delta(H_1$: **5**$)_{SCS}$	1.784	0.012	0.958	3	G(**m**)
2	$\delta(H_8$: **2**$)_{SCS}$ *vs.* $\delta(H_1$: **5**$)_{SCS}$	0.023	0.000	0.995	3	G(**m**)
3	$\delta(H_8$: **3**$)_{SCS}$ *vs.* $\delta(H_1$: **5**$)_{SCS}$	−1.383	0.006	0.980	3	G(**m**)
4	$\delta(H_8$: **4**$)_{SCS}$ *vs.* $\delta(H_1$: **5**$)_{SCS}$	−1.169	−0.022	0.772	3	G(**m**)
5	$\delta(H_8$: **1**$)_{SCS}$ *vs.* $\delta(H_1$: **5**$)_{SCS}$	2.058	0.173	0.9996	4	G(**n**)
6	$\delta(H_8$: **2**$)_{SCS}$ *vs.* $\delta(H_1$: **5**$)_{SCS}$	0.458	−0.015	0.933	4	G(**n**)
7	$\delta(H_8$: **3**$)_{SCS}$ *vs.* $\delta(H_1$: **5**$)_{SCS}$	0.301	−0.034	0.883	4	G(**n**)
8	$\delta(H_8$: **4**$)_{SCS}$ *vs.* $\delta(H_1$: **5**$)_{SCS}$	−0.953	−0.076	0.984	4	G(**n**)
9	$\delta(H_2$: **1**$)_{SCS}$ *vs.* $\delta(H_1$: **5**$)_{SCS}$	−1.227	−0.009	0.954	3	G(**m**)
10	$\delta(H_2$: **2**$)_{SCS}$ *vs.* $\delta(H_1$: **5**$)_{SCS}$	−5.700	−0.036	0.965	3	G(**m**)
11	$\delta(H_2$: **3**$)_{SCS}$ *vs.* $\delta(H_1$: **5**$)_{SCS}$	−5.415	−0.038	0.957	3	G(**m**)
12	$\delta(H_2$: **4**$)_{SCS}$ *vs.* $\delta(H_1$: **5**$)_{SCS}$	−4.078	−0.034	0.942	3	G(**m**)
13	$\delta(H_2$: **1**$)_{SCS}$ *vs.* $\delta(H_1$: **5**$)_{SCS}$	−1.266	−0.093	0.9998	4	G(**n**)
14	$\delta(H_2$: **2**$)_{SCS}$ *vs.* $\delta(H_1$: **5**$)_{SCS}$	−1.854	−0.114	0.9994	4	G(**n**)
15	$\delta(H_2$: **3**$)_{SCS}$ *vs.* $\delta(H_1$: **5**$)_{SCS}$	−0.848	−0.054	0.991	4	G(**n**)
16	$\delta(H_2$: **4**$)_{SCS}$ *vs.* $\delta(H_1$: **5**$)_{SCS}$	−1.677	−0.096	0.995	4	G(**n**)
17	$\delta(H_2$: **2**$)_{SCS}$ *vs.* $\delta(H_2$: **1**$)_{SCS}$	4.591	0.004	0.9993	3	G(**m**)
18	$\delta(H_2$: **3**$)_{SCS}$ *vs.* $\delta(H_2$: **1**$)_{SCS}$	4.401	0.001	1.000	3	G(**m**)
19	$\delta(H_2$: **4**$)_{SCS}$ *vs.* $\delta(H_2$: **1**$)_{SCS}$	3.365	−0.003	0.9991	3	G(**m**)
20	$\delta(H_2$: **2**$)_{SCS}$ *vs.* $\delta(H_2$: **1**$)_{SCS}$	1.464	0.023	0.9996	4	G(**n**)
21	$\delta(H_2$: **3**$)_{SCS}$ *vs.* $\delta(H_2$: **1**$)_{SCS}$	0.670	0.009	0.991	4	G(**n**)
22	$\delta(H_2$: **4**$)_{SCS}$ *vs.* $\delta(H_2$: **1**$)_{SCS}$	1.324	0.028	0.995	4	G(**n**)
23	$\delta(H_2$: **4**$)_{SCS}$ *vs.* $\delta(H_2$: **2**$)_{SCS}$	0.851	0.012	0.996	7	G(**m**+**n**)
24	$\delta(C_i$: **1**$)_{SCS}$ *vs.* $\delta(C_i$: **2**$)_{SCS}$	0.589	−0.42	0.997	7	G(**m**+**n**)
25	$\delta(C_i$: **3**$)_{SCS}$ *vs.* $\delta(C_i$: **2**$)_{SCS}$	1.026	−0.11	0.9991	7	G(**m**+**n**)
26	$\delta(C_i$: **4**$)_{SCS}$ *vs.* $\delta(C_i$: **2**$)_{SCS}$	1.029	−0.18	0.9998	7	G(**m**+**n**)

[a]The constants (*a*, *b*, *r*) are defined by $y = ax + b$ (*r*: correlation coefficient).

[b]G(**m**): Y = H (**a**), OMe (**c**), and Me (**d**); G(**n**): Y = Cl (**f**), Br (**g**), COOEt (**h**), and NO_2 (**j**); G(**m**+**n**): **a**, **c**, **d**, **f**–**h**, and **j**.

(**B**, **pd**) for G(**m**). The *a* values for G(**m**) in the plots of $\delta(H_8$: **1**–**4**$)$ versus $\delta(H_1$: **5**$)$ become smaller monotonically as Z goes from O (**1**), to S (**2**), then to Se (**3**), while that for Z = Te (**4**) is slightly larger than the case of Z = Se (**3**). The results should not be inconsistent with the above conclusion.

As shown in Figure 5, the plots of $\delta(H_2$: **1**–**4**$)$ versus $\delta(H_1$: **5**$)$ are also plotted as two correlations (entries 9–12 for G(**m**) and entries 13–16 for G(**n**) in Table II). However, the observed trends are more complex than the case of $\delta(H_8$: **1**–**4**$)$ versus $\delta(H_1$: **5**$)$. Whereas **5** has the C_s symmetry, **1**–**4** do not. Consequently, H_2 in **1**–**4** must exist in a delicate area of the anisotropic effect: The effect changes depending on the torsional angle between naphthyl and aryl planes and Z. As a result, the *a* values for the plots of $\delta(H_2$: **1**–**4**$)$ versus $\delta(H_1$: **5**$)$ change depending on Z. Nevertheless, the plots are analyzed as two correlations. We believe that the plots of $\delta(H_2$: **1**–**4**$)$ versus $\delta(H_1$: **5**$)$ are the reflection of the (**A**, **pl**) structure for G(**n**) and (**B**, **pd**) for G(**m**), although they would be in equilibrium with each other for Y of electronically neutral substituents.

To confirm the conclusion above, $\delta(H_2$: **2**–**4**$)$ are plotted versus $\delta(H_2$: **1**$)$: The plots shown in Figure 6 are also analyzed as two correlations (entries 17–19 for G(**m**) and entries 20–22 for G(**n**) in Table II). $\delta(H_2$: **2**–**4**$)$ are correlated with $\delta(H_2$: **1**$)$ separately by G(**m**) and

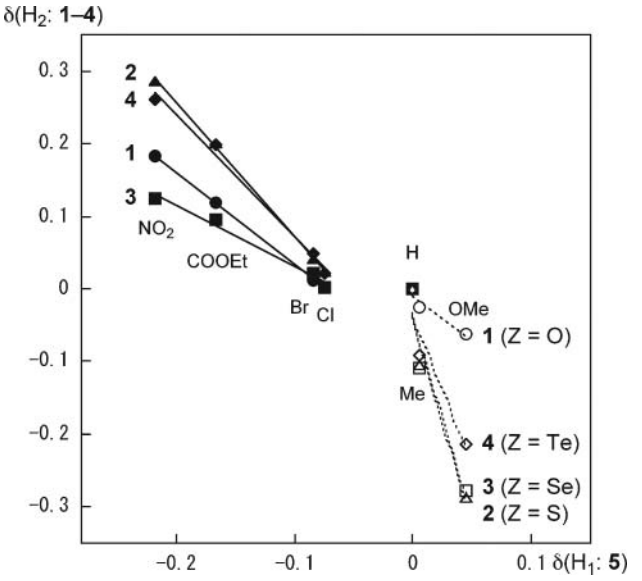

Figure 5 Plots of $\delta(H_2$: **1**–**4**) versus $\delta(H_1$: **5**).

G(**n**). The results show that the structures of **2**–**4** are controlled by Y as observed in **1**. $\delta(H_2$: **4**) are similarly plotted versus $\delta(H_2$: **2**). Figure 7 shows the plot, and the correlation is given in Table II (entry 23). The correlation is very good. The results show that the structure of **4** changes depending on Y very similarly to the case of **2**. The anisotropic conditions for H_2 in **4** must also be very similar to the case of **2**. However, the firm conclusion would be given for **4** if the structure of **4** is determined in crystals.

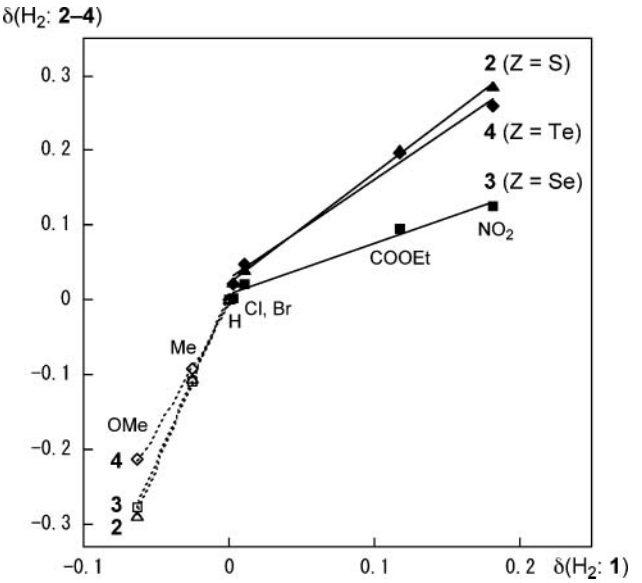

Figure 6 Plots of $\delta(H_2$: **2**–**4**) versus $\delta(H_2$: **1**).

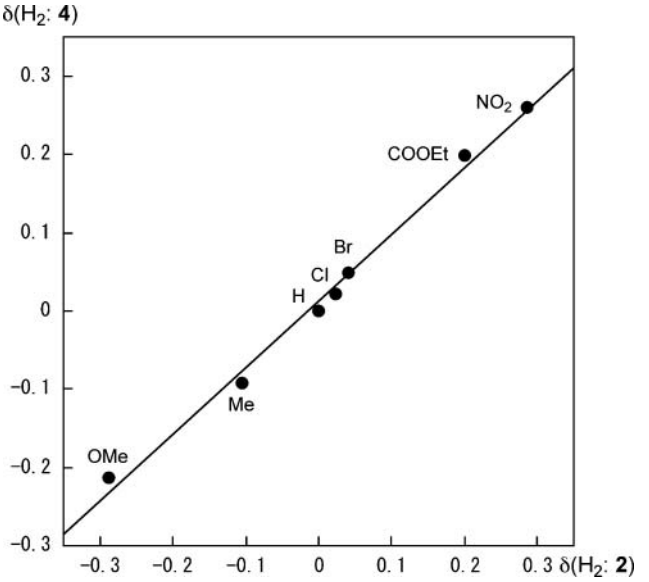

Figure 7 Plot of $\delta(H_2$: **4**) versus $\delta(H_2$: **2**).

Finally, $\delta(C_i$: **1**, **3**, **4**) are plotted versus $\delta(C_i$: **2**). Figure 8 shows the plots. The plots are analyzed as single correlation for each. The correlations (entries 24–26 in Table II) are excellent, especially for **3** and **4**. It is highly interesting that $\delta(C_i$: **1**–**4**) are hardly affected by the conformation around the Z–C_{Ar} bonds irrespective of the large dependence in δ(H: **1**–**4**) and δ(Se: **3**).

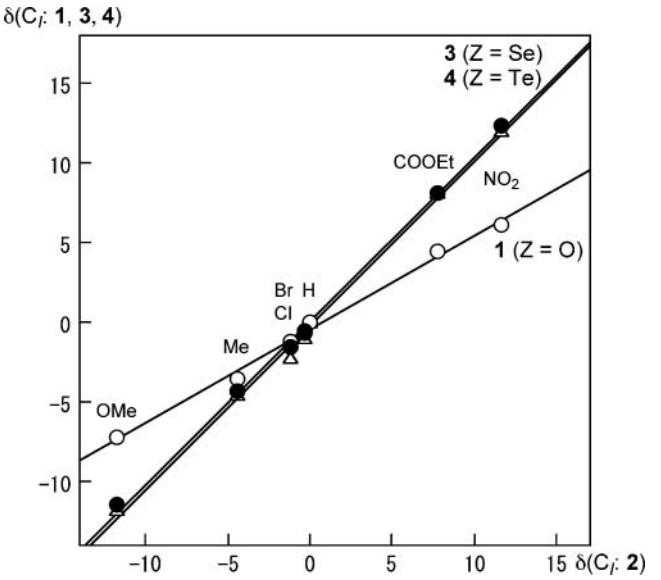

Figure 8 Plots of $\delta(C_i$: **1**, **3**, **4**) versus $\delta(C_i$: **2**).

EXPERIMENTAL

1-(*p*-Bromophenoxy)naphthalene (1g)[11]

Colorless oil; ^{1}H NMR (300 MHz, $CDCl_3$/TMS): δ 6.87–6.93 (m, 2H), 6.96 (dd, $J = 0.9$ and 7.5 Hz, 1H), 7.35–7.44 (m, 3H), 7.45–7.55 (m, 2H), 7.61 (d, $J = 8.3$ Hz, 1H), 7.86–7.89 (m, 1H), 8.18–8.21 (m, 1H); ^{13}C NMR (75 MHz, $CDCl_3$/TMS): δ 114.0, 115.4, 120.0, 121.9, 123.9, 125.8, 126.1, 126.7, 126.8, 127.8, 132.7, 133.1, 135.0, 157.3; anal. Found: C, 64.37; H, 3.57; N, 0.00%; Calcd for $C_{16}H_{11}BrO$: C, 64.24; H, 3.71; N, 0.00%.

1-(*p*-Ethoxycarbonylphenoxy)naphthalene (1h)

Colorless oil; ^{1}H NMR (300 MHz, $CDCl_3$/TMS): δ 1.38 (t, $J = 7.1$ Hz, 3H), 4.35 (q, $J = 7.1$ Hz, 2H), 6.99–7.01 (m, 2H), 7.10 (dd, $J = 0.7$ and 7.5 Hz, 1H), 7.42–7.55 (m, 3H), 7.72 (d, $J = 8.3$ Hz, 1H), 7.84 (d, $J = 7.7$ Hz, 1H), 7.98–8.05 (m, 3H); ^{13}C NMR (75 MHz, $CDCl_3$/TMS): δ 14.3, 60.8, 115.6, 116.8, 121.9, 124.7, 125.8, 126.3, 126.7, 127.0, 127.9, 128.3, 131.7, 135.0, 151.3, 162.4, 166.1; anal. Found: C, 78.01; H, 5.53; N, 0.00%; Calcd for $C_{19}H_{16}O_3$: C, 78.06; H, 5.52; N, 0.00%.

1-(Phenylthio)naphthalene (2a)

Colorless oil; ^{1}H NMR (300 MHz, $CDCl_3$/TMS): δ 7.09–7.22 (m, 5H), 7.40 (dd, $J = 7.2$ and 9.1 Hz, 1H), 7.47 (t, $J = 3.3$ Hz, 1H), 7.50 (t, $J = 3.3$ Hz, 1H), 7.65 (dd, $J = 1.2$ and 7.2 Hz, 1H), 7.83 (t, $J = 5.7$ Hz, 1H), 7.85 (d, $J = 6.3$ Hz, 1H), 8.34–8.40 (m, 1H); ^{13}C NMR (75 MHz, $CDCl_3$/TMS): δ 125.6, 125.8, 126.1, 126.4, 126.9, 128.5, 128.9, 129.0, 129.2, 131.2, 132.5, 133.5, 134.2, 136.9; anal. Found: C, 81.50; H, 5.18; N, 0.01%; Calcd for $C_{16}H_{12}S$: C, 81.31; H, 5.12; N, 0.00%.

1-(*p*-Anisylthio)naphthalene (2c)

Pale yellow needles; mp 109.0–110.0°C; ^{1}H NMR (300 MHz, $CDCl_3$/TMS): δ 3.78 (s, 3H), 6.85 (d, $J = 6.6$ Hz, 2H), 7.32 (d, $J = 6.6$ Hz, 2H), 7.30–7.39 (m, 2H), 7.48–7.57 (m, 2H), 7.73 (dd, $J = 2.4$ and 7.0 Hz, 1H), 7.82–7.88 (m, 1H), 8.34–8.40 (m, 1H); ^{13}C NMR (100 MHz, $CDCl_3$/TMS): δ 55.4, 115.0, 124.9, 125.2, 125.7, 126.3, 126.5, 127.4, 128.5, 128.5, 132.2, 133.8, 134.0, 134.6, 159.4; anal. Found: C, 76.49; H, 5.35; N, 0.00%; Calcd for $C_{17}H_{14}OS$: C, 76.66; H, 5.30; N, 0.00%.

1-(*p*-Tolylthio)naphthalene (2d)

Pale yellow oil; ^{1}H NMR (300 MHz, $CDCl_3$/TMS): δ 2.29 (s, 3H), 7.05 (d, $J = 8.4$ Hz, 2H), 7.16 (d, $J = 8.4$ Hz, 2H), 7.38 (d, $J = 8.4$ Hz, 1H), 7.47–7.56 (m, 3H), 7.79 (d, $J = 8.1$ Hz, 1H), 7.83–7.87 (m, 1H), 8.34–8.40 (m, 1H); ^{13}C NMR (75 MHz, $CDCl_3$/TMS): δ 21.0, 125.4, 125.7, 126.3, 126.7, 128.4, 128.5, 130.0, 130.2, 130.9, 132.5, 132.6, 133.1, 134.1, 136.6; anal. Found: C, 81.57; H, 5.78; N, 0.00%; Calcd for $C_{17}H_{14}S$: C, 81.56; H, 5.64; N, 0.00%.

1-(*p*-Chlorophenylthio)naphthalene (2f)

Pale yellow needles; mp 109.5–110.5°C; ^{1}H NMR (300 MHz, $CDCl_3$/TMS): δ 7.04 (dt, $J = 2.4$ and 8.7 Hz, 2H), 7.13 (dt, $J = 2.4$ and 8.7 Hz, 2H), 7.40 (dd, $J = 7.2$ and 8.4 Hz, 1H), 7.47 (t, $J = 3.3$ Hz, 1H), 7.55 (t, $J = 3.3$ Hz, 1H), 7.68 (dd, $J = 1.2$ and 7.2 Hz, 1H), 7.84 (dd, $J = 3.3$ and 7.5 Hz, 2H), 8.29–8.32 (m, 1H); ^{13}C NMR (75 MHz, $CDCl_3$/TMS): δ 125.5, 125.8, 126.5, 127.1, 128.6, 129.1, 129.6, 129.8, 130.4, 131.9, 133.0, 133.5, 134.3, 135.7; anal. Found: C, 70.81; H, 4.01; N, 0.00%; Calcd for $C_{16}H_{11}ClS$: C, 70.97; H, 4.09; N, 0.00%.

1-(*p*-Bromophenylthio)naphthalene (2g)

Pale yellow needles; mp 73.5–74.0°C; ^{1}H NMR (300 MHz, $CDCl_3$/TMS): δ 6.96 (dt, $J = 2.4$ and 8.7 Hz, 2H), 7.25 (dt, $J = 2.4$ and 8.7 Hz, 2H), 7.34 (dd, $J = 7.2$ and 8.4 Hz, 1H), 7.46 (t, $J = 3.3$ Hz, 1H), 7.49 (t, $J = 3.3$Hz, 1H), 7.69 (dd, $J = 1.2$ and 7.2 Hz, 1H), 7.83 (dd, $J = 3.0$ and 5.7 Hz, 2H), 8.28–8.32 (m, 1H); ^{13}C NMR (75 MHz, $CDCl_3$/TMS): δ 119.7, 125.5, 125.8, 126.6, 127.2, 128.7, 129.8, 129.9, 130.1, 132.0, 133.3, 133.6, 134.3, 136.6; anal. Found: C, 60.97; H, 3.50; N, 0.00%; Calcd for $C_{16}H_{11}BrS$: C, 60.96; H, 3.52; N, 0.00%.

1-(*p*-Ethoxycarbonylphenylthio)naphthalene (2h)

Colorless needles; mp 84.0–85.0°C; ^{1}H NMR (300 MHz, $CDCl_3$/TMS): δ 1.24 (t, $J = 7.2$ Hz, 3H), 4.22 (q, $J = 7.2$ Hz, 2H), 6.96 (dt, $J = 2.1$ and 8.7 Hz, 2H), 7.37–7.46 (m, 3H), 7.74 (dt, $J = 2.1$ and 8.7 Hz, 2H), 7.76–7.83 (m, 2H), 7.85 (d, $J = 8.4$ Hz, 1H), 8.22–8.30 (m, 1H); ^{13}C NMR (100 MHz, $CDCl_3$/TMS): δ 29.7, 60.8, 125.8, 125.9, 126.3, 126.7, 127.3, 127.4, 128.4, 128.7, 130.0, 130.7, 134.1, 134.4, 134.9, 144.7, 166.3; anal. Found: C, 73.71; H, 5.23; N, 0.04%; Calcd for $C_{19}H_{16}O_2S$: C, 74.00; H, 5.23; N, 0.00%.

1-(*p*-Nitrophenylthio)naphthalene (2j)

Yellow needles; mp 92.0–93.0°C; ^{1}H NMR (300 MHz, $CDCl_3$/TMS): δ 7.04 (dt, $J =$ 2.4 and 9.0 Hz, 2H), 7.50–7.60 (m, 3H), 7.81 (dd, $J = 0.9$ and 7.2 Hz, 1H), 7.92–8.00 (m, 3H), 8.26 (d, $J = 8.7$ Hz, 1H), 8.22 (d, $J = 9.0$ Hz, 1H); ^{13}C NMR (100 MHz, $CDCl_3$/TMS): δ 124.0, 125.5, 125.9, 126.0, 126.7, 126.9, 127.8, 128.9, 131.5, 134.1, 134.5, 135.8, 145.1, 148.5; anal. Found: C, 68.25; H, 3.97; N, 4.93%; Calcd for $C_{16}H_{11}NO_2S$: C, 68.31; H, 3.94; N, 4.98%.

1-(Phenyltelluro)naphthalene (4a)

Colorless oil; ^{1}H NMR (300 MHz, $CDCl_3$/TMS): δ 7.09–7.22 (m, 3H), 7.25 (t, $J =$ 7.7 Hz, 1H), 7.44–7.51 (m, 2H), 7.59 (t, $J = 1.3$ and 6.8 Hz, 2H), 7.76 (dd, $J = 2.9$ and 4.6 Hz, 1H), 7.80 (d, $J = 8.1$ Hz, 1H), 7.97 (dd, $J = 1.1$ and 7.0 Hz, 1H), 8.12–8.21 (m, 1H); anal. Found: C, 57.85; H, 3.70; N, 0.00%; Calcd for $C_{16}H_{12}Te$: C, 57.91; H, 3.64; N, 0.00%.

1-(*p*-Anisyltelluro)naphthalene (4c)

Colorless needles; mp 71.0–72.0°C; ^{1}H NMR (300 MHz, $CDCl_3$/TMS): δ 3.79 (s, 3H), 6.79 (d, $J = 8.7$ Hz, 2H), 7.25 (dd, $J = 7.5$ and 7.8 Hz, 1H), 7.47–7.56 (m, 2H), 7.74 (d, $J = 9.0$ Hz, 2H), 7.75–7.82 (m, 3H), 8.06–8.09 (m, 1H); ^{13}C NMR (75 MHz, $CDCl_3$/TMS): δ 55.1, 102.9, 115.6, 118.8, 126.2, 126.5, 126.7, 128.6, 128.7, 130.7, 133.7, 135.4, 136.4, 140.9, 160.0; anal. Found: C, 56.51; H, 3.82; N, 0.00%; Calcd for $C_{17}H_{14}OTe$: C, 56.42; H, 3.90; N, 0.00%.

1-(*p*-Tolyltelluro)naphthalene (4d)

Colorless oil; ^{1}H NMR (300 MHz, $CDCl_3$/TMS): δ 2.31 (s, 3H), 7.01 (d, $J = 7.9$ Hz, 2H), 7.25 (dd, $J = 7.0$ and 8.1 Hz, 1H), 7.45–7.53 (m, 2H), 7.57 (d, $J = 7.9$ Hz, 2H), 7.76–7.81 (m, 2H), 7.88 (dd, $J = 1.1$ and 7.2 Hz, 1H), 8.07–8.12 (m, 1H); ^{13}C NMR (75 MHz, $CDCl_3$/TMS): δ 20.2, 110.2, 118.2, 126.5, 126.8, 128.7, 129.0, 130.3, 130.5, 131.3, 133.7, 135.7, 137.9, 138.0, 138.3; anal. Found: C, 59.15; H, 4.10; N, 0.00%; Calcd for $C_{17}H_{14}Te$: C, 59.03; H, 4.08; N, 0.00%.

1-(*p*-Chlorophenyltelluro)naphthalene (4f)

Colorless oil; ^{1}H NMR (300 MHz, $CDCl_3$/TMS): δ 7.12 (d, $J = 8.6$ Hz, 2H), 7.31 (dd, $J = 7.2$ and 8.3 Hz, 1H), 7.50 (d, $J = 8.4$ Hz, 2H), 7.48–7.54 (m, 2H), 7.79–7.84 (m, 1H), 7.87 (d, $J = 8.3$ Hz, 1H), 7.99 (dd, $J = 1.1$ and 7.0 Hz, 1H), 8.12–8.18 (m, 1H); ^{13}C NMR (75 MHz, $CDCl_3$/TMS): δ 112.5, 117.4, 126.4, 126.5, 127.1, 128.8, 129.6, 129.8, 131.7, 133.6, 134.0, 135.7, 138.4, 139.1; anal. Found: C, 52.55; H, 3.10; N, 0.00%; Calcd for $C_{16}H_{11}ClTe$: C, 52.46; H, 3.03; N, 0.00%.

1-(*p*-Bromophenyltelluro)naphthalene (4g)

Colorless needles; mp 72.0–73.0°C; ^{1}H NMR (300 MHz, $CDCl_3$/TMS): δ 7.24 (d, $J = 8.4$ Hz, 2H), 7.29 (dd, $J = 7.2$ and 8.3 Hz, 1H), 7.40 (d, $J = 8.4$ Hz, 2H), 7.46–7.53 (m, 2H), 7.77–7.82 (m, 1H), 7.85 (d, $J = 8.3$ Hz, 1H), 8.02 (dd, $J = 1.3$ and 7.2 Hz, 1H), 8.12–8.17(m, 1H); ^{13}C NMR (75 MHz, $CDCl_3$/TMS): δ 113.7, 117.3, 122.2, 126.4, 126.5, 127.2, 128.9, 130.0, 131.7, 132.6, 133.7, 135.8, 138.6, 139.3; anal. Found: C, 46.65; H, 2.76; N, 0.00%; Calcd for $C_{16}H_{11}BrTe$: C, 46.78; H, 2.70; N, 0.00%.

1-(*p*-Ethoxycarbonylphenyltelluro)naphthalene (4h)

Colorless needles; mp 76.5–77.0°C; ^{1}H NMR (300 MHz, $CDCl_3$/TMS): δ 1.34 (t, $J = 7.2$ Hz, 3H), 4.32 (q, $J = 7.2$ Hz, 2H), 7.35 (dd, $J = 7.3$ and 8.4 Hz, 1H), 7.46–7.54 (m, 4H), 7.75 (d, $J = 8.4$ Hz, 2H), 7.81–7.86 (m, 1H), 7.93 (d, $J = 8.3$ Hz, 1H), 8.17 (dd, $J = 1.5$ and 7.2 Hz, 1H), 8.19–8.23 (m, 1H); anal. Found: C, 56.25; H, 3.93; N, 0.00%; Calcd for $C_{19}H_{16}O_2Te$: C, 56.50; H, 3.99; N, 0.00%.

1-(*p*-Nitrophenyltelluro)naphthalene (4j)

Yellow needles; mp 111.0–111.5°C; ^{1}H NMR (300 MHz, $CDCl_3$/TMS): δ 7.41 (dd, $J = 7.2$ and 8.3 Hz, 1H), 7.46 (d, $J = 8.8$ Hz, 2H), 7.50–7.57 (m, 2H), 7.83–7.87 (m, 1H),

7.89 (d, $J = 8.8$ Hz, 2H), 8.00 (d, $J = 8.1$ Hz, 1H), 8.19–8.26 (m, 1H), 8.28 (dd, $J = 1.3$ and 7.0 Hz, 1H); ^{13}C NMR (75 MHz, $CDCl_3$/TMS): δ 115.9, 119.3, 123.6, 126.7, 126.7, 127.7, 129.0, 131.3, 132.3, 133.8, 134.6, 135.9, 141.8, 146.9; anal. Found: C, 50.89; H, 2.98; N, 3.80%; Calcd for $C_{16}H_{11}NO_2Te$: C, 50.99; H, 2.94; N, 3.72%.

X-Ray Structural Determination

The single crystals of **1a**, **1c**, **2c**, and **2g** were measured on a Rigaku AFC-5R automated four-circle diffractometer with graphite monochromated Mo Kα radiation ($\lambda = 0.71069$ Å) and a rotating anode generator at 292–298 K. The structures were solved by direct methods [SAPI90[14] for **1a**, SAPI91[15] for **1c**, and DIRDIF92 (PATTY)[16] for **2c** and **2g**] and expanded using Fourier techniques (teXsan[17]). The nonhydrogen atoms were refined anisotropically. Hydrogen atoms were included but not refined. The final cycle of full-matrix least-squares refinement was based on F^2. All calculations were performed using the teXsan crystallographic software package.[17]

Deposition number CCDC-711230 for **1a**, CCDC-711231 for **1c**, CCDC-711232 for **2c**, and CCDC-711233 for **2g** contain the supplementary crystallographic data for this article. These data can be obtained free of charge from the Cambridge Crystallographic Data Centre via www.ccdc.cam.ac.uk/data request/cif.

REFERENCES

1. (a) A. Wakamiya, K. Mishima, K. Ekawa, and S. Yamaguchi, *Chem. Commun.*, 579–581 (2008); (b) S. Yamaguchi, T. Shirasaka, S. Akiyama, and K. Tamao, *J. Am. Chem. Soc.*, **124,** 8816–8817 (2002); (c) S. Yamaguchi, S. Akiyama, and K. Tamao, *J. Am. Chem. Soc.*, **123,** 11372–11375 (2001).
2. W. Nakanishi, S. Hayashi, and T. Uehara, *Eur. J. Org. Chem.*, 3933–3943 (2001).
3. (a) W. Nakanishi, S. Hayashi, D. Shimizu, and M. Hada, *Chem. Eur. J.*, **12,** 3829–3846 (2006); (b) S. Hayashi and W. Nakanishi, *Bioinorg. Chem. Applic.*, 1–13, doi:10.1155/BCA/2006/79327 (2006).
4. S. Hayashi, K. Yamane, and W. Nakanishi, *J. Org. Chem.*, **72,** 7587–7596 (2007).
5. T. Nakamoto, S. Hayashi, and W. Nakanishi, *J. Org. Chem.*, **73,** 9259–9269 (2008).
6. (a) S. Hayashi and W. Nakanishi, *J. Org. Chem.*, **64,** 6688–6696 (1999); (b) W. Nakanishi, S. Hayashi, and H. Yamaguchi, *Chem. Lett.*, 947–948 (1996).
7. (a) W. Nakanishi, S. Hayashi, A. Sakaue, G. Ono, and Y. Kawada, *J. Am. Chem. Soc.*, **120,** 3635–3640 (1998); (b) W. Nakanishi and S. Hayashi, *J. Org. Chem.*, **67,** 38–48 (2002).
8. W. Nakanishi, S. Hayashi, and T. Uehara, *J. Phys. Chem. A*, **103,** 9906–9912 (1999).
9. S. Hayashi, H. Wada, T. Ueno, and W. Nakanishi, *J. Org. Chem.*, **71,** 5574–5585 (2006).
10. Structures of 9-(arylselanyl)triptycenes (**7**: 9-(*p*-YC_6H_4Se)Tpc) are also demonstrated to be **pl** for the aryl groups in crystals and solutions. The Se atom of **7** is attached to the sp^3 carbon of the triptycyl group, whereas the atom bonds to the sp^2 carbon in each of **1**–**6**. Therefore, it would be more reasonable to employ NMR data of **5** and **6** to determine the structures of **1**–**4** in solutions.
11. R. G. R. Bacon and O. J. Stewart, *J. Chem. Soc.*, 4953–4961 (1965).
12. The X-ray crystallographic analysis could not be carried out for **1f**, **1g**, and **1h** because of their oily property at ambient temperatures around 24°C. The single crystal of **1j** was too thin to determine its structure by the X-ray crystallographic analysis.
13. The plot versus δ(Se: **5**)$_{SCS}$ is analyzed by two groups: Data with Y = NMe_2, OMe, Me, and H make a group, and those with Y = NO_2, CN, COOEt, Br, Cl, and F belong to another. Correlations are poor for the plot versus δ(Se: **6**)$_{SCS}$. The structure of **3** could be (**A**, **pl**) for Y = NO_2, CN, COOEt, Br, Cl, and F in solutions. However, the correlation must be carefully examined, since

the intercepts for the correlations are –3.1 to –4.3, which are not close to 0.0 (see entries 6 and 8 in Table II), which lead the conclusions in the text.
14. H.-F. Fan, Structure Analysis Programs with Intelligent Control, Rigaku Corporation, Tokyo, Japan (1990).
15. H.-F. Fan, Structure Analysis Programs with Intelligent Control, Rigaku Corporation, Tokyo, Japan (1991).
16. P. T. Beurskens, G. Admiraal, G. Beurskens, W. P. Bosman, R. de Gelder, R. Israel, and J. M. M. Smits, The DIRDIF-94 program system, Technical Report of the Crystallography Laboratory, University of Nijmegen, The Netherlands (1994).
17. Single Crystal Structure Analysis Software, Version 1.7. Molecular Structure Corporation, MSC, The Woodlands, TX, USA (1995).